Colloids and Surfaces A: Physicochem. Eng. Aspects 365 (2010) 181–188

Contents lists available at ScienceDirect

Colloids and Surfaces A: Physicochemical and Engineering Aspects

journal homepage: www.elsevier.com/locate/colsurfa

# On the use of electrical conductance measurements for the stability of oil-in-water Pickering emulsions

E.-M. Varka[a], C. Ampatzidis[a], M. Kostoglou[a], T. Karapantsios[a,*], V. Dutschk[b]

[a] Dept. Chemistry, Aristotle University of Thessaloniki, University Box 166, 541 24 Thessaloniki, Greece
[b] Leibniz Institute of Polymer Research, Dresden, Germany

ARTICLE INFO

*Article history:*
Received 29 October 2009
Received in revised form 8 February 2010
Accepted 14 February 2010
Available online 20 February 2010

*Keywords:*
Pickering emulsions
Electrical conductance
Microscopy
Creaming index

ABSTRACT

Non-intrusive and continuous (on-line) techniques for the assessment of emulsion stability are of increasing interest. In this context, this work examines the potential of a new electrical technique (non-intrusive/continuous) against two traditional techniques, an optical technique (intrusive/intermittent) and a volumetric technique (non-intrusive/intermittent), for the assessment of the stability of Pickering emulsions. Surface modified hydrophilic particles (OS1, Sasol) were employed in making O/W Pickering emulsions. Experiments were performed with different water/oil volume ratios and particles concentrations. Emulsions stability was registered simultaneously by: (i) Electrical conductance signals taken continuously at a certain height inside the test vessel for determining the evolution of the local water fraction. (ii) Microscopy photos of samples withdrawn at regular intervals from the test vessel at the same height as electrical measurements for determining the evolution of the local droplet size distribution. (iii). Global volumetric measurements of the different phases (water, oil, emulsion) inside the test vessel made at regular intervals for determining the evolution of the location of the phases separation interface. Analysis of the results of each technique and comparisons among them are presented and discussed in detail.



## 1. Introduction

Emulsions are omnipresent. They dominate our daily life ranging from cosmetic products over foods, cleaning, pharmaceutical products to paint and oil industries [1]. Emulsions are heterogeneous mixtures consisting of at least two immiscible liquids [2]. The dispersed phase is present in the form of droplets in a continuous phase. Liquid/liquid immiscibility creates an interfacial tension at the contact area between the two liquids. As a consequence emulsions are thermodynamically unstable systems since the increase in the interfacial contact area results in an increase in chemical potential. In thermodynamic terms the free energy penalty of emulsion can be reduced by the use of surface active agents components (surfactants), amphiphilic polymers or proteins, which sufficiently reduce interfacial tension [3].

The relative hydrophilic–lipophilic balance of these molecules is known to be the most important parameter dictating the emulsion type oil-in-water (O/W) or water-in-oil (W/O) [4]. However, surfactants introduce complexities some times while trying to interpret their role, because of their incorporation into oil and water. In this regard, surfactant-free emulsions are one of the most adequate systems for scrutiny.

The so-called Pickering emulsions or more generally solid-stabilized emulsions, can be obtained with a wide variety of organic or mineral powders such as latex, silica, aluminum, and clays. Although such emulsions have been studied since the beginning of this century [5,6] their mechanism of destabilization is still under investigation. Some general rules concerning Pickering emulsions that arise from the different studies reported in the literature [7,8], are the following: (i) the continuous phase of the preferred emulsion is normally the one in which the particles are preferentially dispersed; (ii) the particle surfaces must be partially wettable by both oil and water. This latter condition implies that the contact angle of the three-phase system must be greater than 0° and less than 180°. More specifically, for O/W emulsions particles with contact angles below 90° are preferred whereas for W/O emulsions a contact angle of above 90° is crucial. A convenient way to tailor contact angles is by mixing particles with surfactants [9,10].

The study of solid-stabilized emulsions has entered a very fruitful period and in this paper we aim to present a new non-intrusive method capable of registering their destabilization process. Several methods have been employed in the past, e.g. light scattering, laser diffraction, optical microscopy, to investigate the progress of emulsification which determine droplets size from either direct

* Corresponding author at: Dept. Chemistry, Aristotle University of Thessaloniki, University Box 116, 541 24 Thessaloniki, Greece. Tel.: +30 2310 99 7772; fax: +30 2310 99 7772.
*E-mail address:* karapant@chem.auth.gr (T. Karapantsios).

0927-7757/$ – see front matter © 2010 Elsevier B.V. All rights reserved.
doi:10.1016/j.colsurfa.2010.02.017

visual observations, or from measurements performed on withdrawn samples [11–15]. These methods are limited by the fact that they provide information of droplet sizes only from places where there is either visual access or a sampling mechanism can be inserted. Additionally, the often required significant dilution of samples before measurement can modify some of the emulsion characteristics (e.g. destroy flocks or aggregates). Moreover, these methods cannot provide information on phase volume fraction distributions.

Electrical techniques appear to be a tempting option for measuring non-intrusively the temporal evolution of local volume fractions inside emulsions (opaque or transparent). Such techniques have been used in the past for monitoring other applications such as mixing [16], bubble columns [17], multiphase flows [18,19], solid–liquid filtration [20], and polymerization reactors [21]. A pair of ring electrodes running the internal circumference of a vessel and separated by a certain distance in the axial direction constitutes a probe which, apart from being non-intrusive, is particularly sensitive to phase distribution patterns in the cylindrical segment between the ring electrodes [22]. Ring electrodes have been successfully applied to a number of multi phase applications, e.g. [23,24]. Recently, an upgraded version of the technique has been used for monitoring foam drainage [25,26]. It has been reported that in cases of radially homogeneous dispersions the separation distance between electrodes can be significantly reduced in favor of more localized (axially) measurements.

To our knowledge there has been no systematic use of electrical measurements for studying the phases' distribution in emulsions. In other words, to measure the evolution of local volume fractions during emulsion preparation or destabilization. Some papers used conductance measurements more as an indicator of global emulsion condition rather than as a tool for determining local volume fractions [27–29]. Recently, Kalogianni et al. [30] employed ring electrodes placed at different axial locations of a container to continuously register variations of the local phase volume fractions along the height of the emulsion in a tomographic fashion. Their measurements covered only the emulsion preparation stage and not the subsequent destabilization.

In the present work, we examine the application of a non-intrusive, continuous monitoring, electrical conductance technique for monitoring the evolution of local phase volume fraction inside opaque oil-in-water (O/W) Pickering emulsions during destabilization. The structure of the work is as follows. The experimental set-up and procedures are described first. Results from the three simultaneous techniques (electrical, volumetric, optical) are presented next. An analysis of electrical signals to obtain average droplet sizes follows. Finally, results are compared to each other and discussed in an effort to explain the underlying phenomena.

## 2. Materials and methods

### 2.1. Materials

Oil-in-water Pickering emulsions were prepared using a NaCl aqueous solution, Miglyol oil and hydrophilic particles as stabilizer. Aqueous solution was prepared by dissolving NaCl at a concentration of 0.3 g/l into Millipore filtered water. After salt dissolution the electrical conductivity of the aqueous solution was 125 μS/cm, a value common for tap water. Miglyol 812 oil is a neutral oil (CHG. 071 130, SASOL) typically used in cosmetics and pharmaceuticals.

Hydrophilic particles modified with p-toluene sulfonic acid (OS1, SASOL), were used as received. A relatively wide particle size distribution was found in dispersion with an average size between 60 and 90 nm. OS1 particles have a finite porosity with a BET surface area of 112 $m^2$/g. Besides micro-pores, the strong hysteresis of nitrogen adsorption isotherms indicates the existence of meso-pores in OS1 aggregates. This complex geometry of particle pore spaces makes the estimation of particles' wetting properties extremely difficult. Using a modified Wilhelmy plate method, the average advancing and receding contact angles – corrected according to the Wenzel equation – were 62° and 61°, respectively. Zeta potential of OS1 particles was measured in $10^{-3}$ M KCl solution using a Zetasizer Nano 3000 (Malvern, UK). OS1 particles were positively charged in a broad range of pH values, having the isoelectric point at pH = 9. The stability of particles' surface modification was examined by charge compensating polyelectrolyte titration with a particle charge detector PCD 02 (Mütek, Germany). After several 'washing' cycles, the surface charge was still positive, indicating the surface modification stability. Surface charge quantification was not possible.

**Table 1**
Oil-to-water volume ratios and concentration of OS1 particles in the water phase used for emulsion preparation. √ denotes conditions where emulsion destabilization occurred in reasonable time (less than 5 h).

| OS1 particles (w/w) | Miglyol/water (v/v) | |
|---|---|---|
| | 20/80 | 40/60 |
| 0.1% | √ | √ |
| 0.5% | √ | √ |
| 1% | √ | √ |
| 2.5% | √ | Very stable emulsion |

The employed water/oil volume ratios and particles concentrations are displayed in Table 1.

### 2.2. Procedures for emulsion preparation and destabilization

Emulsions were prepared by intense mechanical agitation (whipping) with a coffee creamer. The impeller of the coffee creamer was placed at the central axis of a Plexiglas taper vessel (Fig. 1) 1.5 cm above the bottom of the vessel. The creamer motor was connected to a variable voltage potentiometer in order to adjust the rotation speed. Destabilization of emulsions was examined inside a cylindrical Plexiglas vessel having 11 cm height and

**Fig. 1.** Emulsification set-up. Coffee creamer is on top with Plexiglas taper vessel underneath.

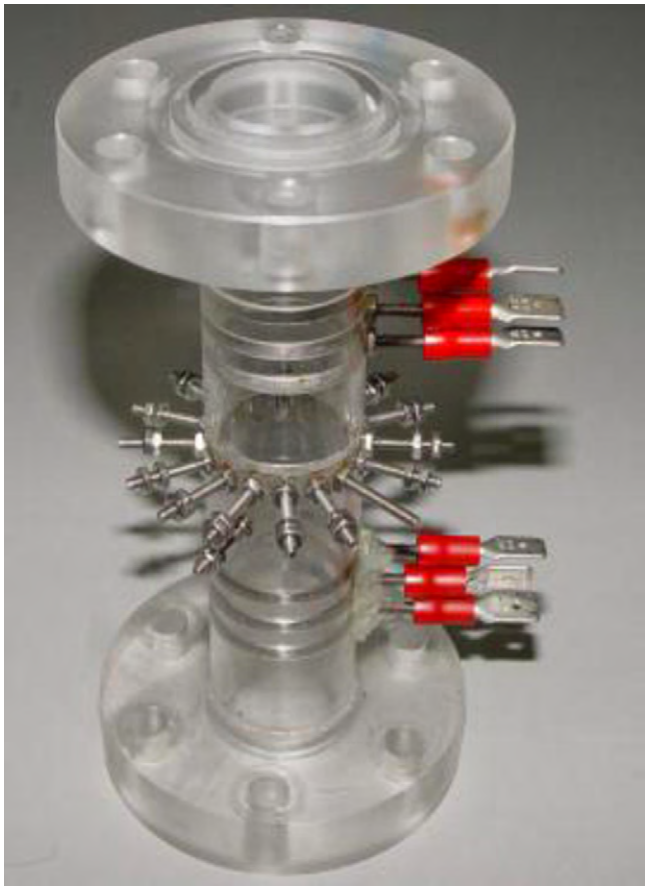

**Fig. 2.** Emulsion destabilization test vessel furnished with several electrodes. Only the pair consisting of the first and third ring electrodes (from the bottom) is used in this study.

2.1 cm internal diameter (Fig. 2). The vessel was designed for electrical tomography measurements and for this it was furnished with several stainless steel electrodes. All electrodes were carefully machined to be flush mounted to the inner wall of the vessel in order to avoid disturbing the emulsions. For the present experiments only one pair of ring electrodes (0.2 cm width) was employed as a measuring probe. These electrodes were 1.05 cm apart from each other (half of the internal diameter of the vessel selected on electrical field considerations [22,25]) and were placed at the lower part of the vessel with the lower electrode at 0.9 cm above the bottom of the vessel. The free surface of the emulsion was ~8 cm above the bottom of the vessel.

Initially, the taper vessel was filled with the appropriate volume of alkaline aqueous solution and load of OS1 particles. The value of the aqueous solution volume was different for different hexane/water volume ratios so as to have always a final volume of 60 ml of oil and water in the emulsion. The coffee creamer was operated at 1260 rpm, a speed adequate to agitate and emulsify the mixture without vortexing and air suction. Agitation was performed in eight sequential runs of 1 min each (8× 1 min). This scheme proved sufficient to achieve stable conditions with the electrical signal reaching a plateau value. Then, the appropriate volume of Miglyol 812 was introduced in the vessel and agitated at 1260 rpm for 4× 1 min. After the end of the emulsification period, the produced emulsion was split into four parts. A first, large part (28 ml) was decanted into the Plexiglas test vessel (Fig. 2) for electrical conductance measurements during destabilization. Second, a 0.5 ml sample was carefully withdrawn from the taper vessel from the region between electrodes using a 5 mm i.d. tube (wide enough to prevent droplets jamming) and was added to a 20% (w/v) Tween 80 solution to prevent droplets coalescence. The sample was then put under a microscope (AxionStar) which was coupled with a digital camera (CANON, PowerShot A640, 10 Megapixels). Finally, two other parts of the emulsion (~10 ml) were decanted into two small glass containers (i.d. 1.6 cm) for taking global photographs of the whole emulsion volume from which the height of the two separating phases was detected with respect to time. One may wonder why phase separation was not monitored directly in the Plexiglas vessel of electrical measurements. The reason was that Plexiglas was not so transparent for taking clear images as glass. This was worse with the emulsion inside the vessel because of the different wetting properties of water and oil against Plexiglas.

### 2.3. Water volumetric fraction from electrical measurements

Electrical conductance data were taken throughout the destabilization process. The technique has been presented in detail elsewhere [25], only a few essential elements are repeated here. An a.c. carrier voltage of $0.250V_{RMS}$ was applied across each electrode pair at a frequency of 25 kHz. This frequency allows suppressing undesirable electrode polarization and capacitive impedance. The response of each probe was fed to an electronic analyzer–demodulator. The analog d.c. output signal of the analyzer from the different probes was acquired at a rate of 1 Hz with the aid of a data acquisition card (ADAM 4018, Advantec) interfaced to a PC. The acquired d.c. signals were then converted to apparent conductance $K_{app}$ (the inverse of apparent resistance) of the emulsion using a calibration curve based on precision resistors. Assuming a uniform dispersion of oil in water inside the measuring volume of each probe, the following holds:

$$\left(\frac{K_{dis}^{app}}{K_{aq}^{app}}\right) = \frac{\sigma_{dis}}{\sigma_{aq}} \quad (1)$$

where $K_{dis}^{app}$ and $\sigma_{dis}$ denote the apparent conductance and conductivity of the dispersion whereas $K_{aq}^{app}$ and $\sigma_{aq}$ denote the apparent conductance and conductivity of the aqueous phase. The normalization of conductance measurements with respect to the conductance of the aqueous phase eliminates errors owing to variations of water conductivity. The normalized conductivity measurements were then transformed into water volumetric fractions ($f_w$) using the equation of Bruggeman (assuming non-conducting oil phase) which is quite popular for emulsion applications, e.g. [29,30]:

$$\sigma_{dis} = \sigma_{aq}(f_w)^{3/2} \quad (2)$$

### 2.4. Creaming index from volumetric measurements

A still digital camera was employed to take photographs of the entire containers with respect to time during emulsion destabilization. These images were used to determine the instantaneous heights of the emulsion and of the aqueous phase inside the containers and from these values estimate the creaming index according to the formula (Fig. 3):

$$CI = \frac{H_{aq}}{H_{tot}} \times 100 \quad (3)$$

The creaming index represents the global volumetric water fraction. It is a measure of the progress of droplet separation as a result of buoyant movement, flocculation and coalescence.

### 2.5. Droplets size from microscopy photos

Several photos were taken by the microscope from different parts of the withdrawn samples until a population above 300

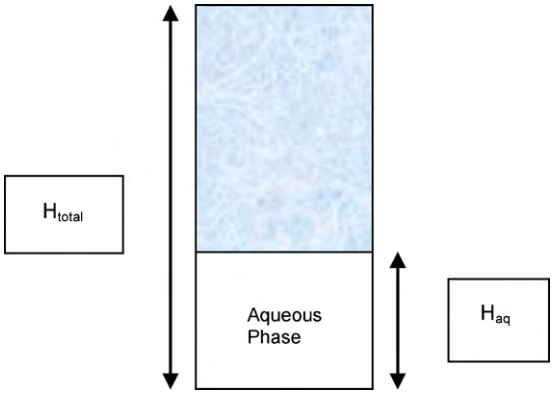


**Fig. 3.** Schematic representation of creaming index estimation.

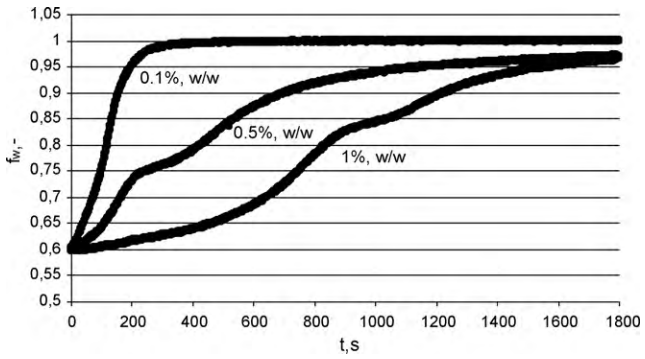


**Fig. 5.** Water fraction ($f_w$) as a function of time ($t$) during destabilization of oil-in-water Pickering emulsions with 40/60 (v/v) oil/water volume ratio and different OS1 particle concentrations.

droplets was collected for each sample in order to ensure statistical significance in the determination of droplets size. A custom-made software capable of handling even very dense emulsions [31] was employed to obtain droplet diameter distributions and from them to calculate the Sauter average droplet diameter (defined as the ratio of the 3rd to the 2nd distribution moment).

## 3. Experimental results

### 3.1. Water volumetric fraction

Fig. 4 presents electrical measurements of local water volume fraction versus time obtained during the destabilization process of 20/80 (v/v) Miglyol-in-water Pickering emulsion at different OS1 particles concentrations. Water fraction starts from 0.8 at $t = 0$ s which corresponds to a well-mixed homogeneous emulsion (at the end of emulsification) and changes towards 1 which corresponds to pure water since the measuring probe is located low in the emulsion. The curves are different but there is a common feature: a fast rise at the beginning which soon turns into a slower rise at longer times. It is most likely that the initial fast rise corresponds to large oil droplets that separate rapidly from the aqueous phase whereas the slow rise corresponds to small droplets that take longer to destabilize. By increasing the OS1 particles concentration from 0.1% to 2.5% the situation changes progressively towards a more stable emulsion. The slopes of the curves reflect the above. The least stable emulsion (0.1%) exhibits the steepest slope whereas the most stable emulsion (2.5%) the gentlest slope. Intermediate particles concentrations correspond to intermediate slopes in a correct qualitative order. Interestingly, the variation of slopes is not proportional to the variation of particles concentration, an indication of the complexity of the system. It seems that as particles concentration increases droplet size decreases (produced during emulsification) yielding more stable emulsions and smaller slopes. Of course, if droplet size decreases at constant oil volume this means higher interfacial area but the increased number of particles appears to overwhelm the effect of the increased interfacial area. In other words, at higher particles concentration small droplets produced during emulsification are better covered and protected by particles against coalescence so smaller droplets survive in the emulsion (see also Section 5).

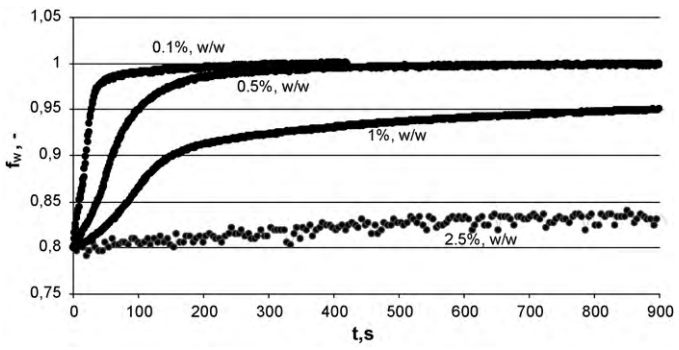


**Fig. 4.** Water fraction ($f_w$) as a function of time ($t$) during destabilization of oil-in-water Pickering emulsions with 20/80 (v/v) oil/water volume ratio and different OS1 particle concentrations.

Fig. 5 presents measurements of local water volumetric fraction versus time obtained during the destabilization process of 40/60 (v/v) Miglyol-in water Pickering emulsion at different OS1 particles concentrations. The arguments made with respect to Fig. 5 hold also here. Only that now the water fraction at the beginning is 0.6 corresponding once more to a homogeneous mixture and that the curve for 2.5% (w/w) particles concentration is omitted because the emulsion is so stable that no variation of the electrical signal is measured in 5 h. Again, two main slopes are observed that can be assigned to two different main droplet sizes. For particles concentration 0.5% and 1% (w/w)/a small "hump" is noticed in the measured curves. This is observed in all repeatability runs but at different moments along the curves. During this phenomenon, we observe visually through the transparent vessel wall a rapid buoyant movement in the emulsion as if a large drop or a large stable flock of small droplets is rising faster than the rest. Unfortunately, the emulsion is opaque so we cannot see deep inside the vessel. It is believed that these complications are due to structural effects emerging from the high volume fraction of the oil in the emulsion and the existence of the particles (this explains why the complications are more pronounced as oil and solids fractions increases).

In a subsequent section it will be shown that the existence of two main slopes in the shape of the water volume fraction curves implies an approximate bidisperse size distribution of droplets. Yet, the curves present additional complications. For example, a third slope appears at the beginning of the curves which is smaller that the first main steep slope. For equal solids load, this third slope lasts longer in the 40/60 emulsions than in the 20/80 emulsions. We believe that this slope is the combined effect of droplets entering the measuring volume of the electrical probe from below and other droplets exiting the measuring volume to above. This notion is supported by electrical curves obtained at the preliminary stage of this work with probes at different heights along the test vessel where it was seen that the lower the location of a probe in the vessel the shorter the initial small slope. However, phenomena such as rearrangement of voids between droplets and subsequent opening of space for the motion of large droplets may also a play a role.

Fig. 6 compares the curves of the two series of Pickering emulsions with different oil/water ratios when particles concentrations

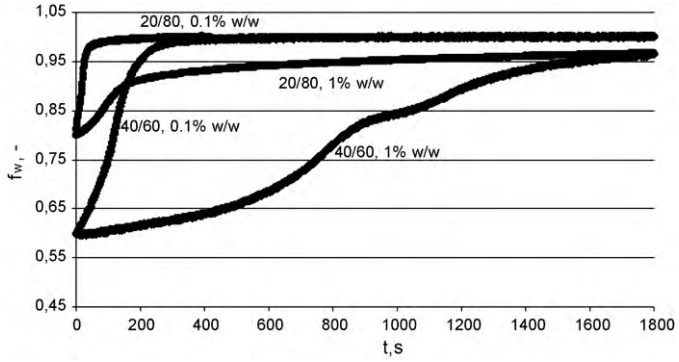


**Fig. 6.** Comparison of water fraction ($f_w$) as a function of time ($t$) during destabilization of oil-in-water Pickering emulsions with 40/60 and 20/80 oil/water volume ratio and different OS1 particle concentrations.

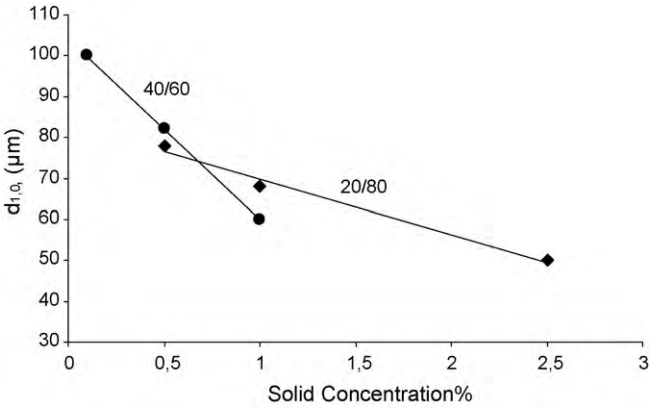


**Fig. 8.** Effect of OS1 particles concentration in Sauter mean droplet diameter.

are the same. As the emulsion gets richer in oil it gets also more stable. This is more evident as particles concentration increases. Based on arguments advanced above, these comments are rather as expected.

### 3.2. Creaming index

Fig. 7 presents the computed creaming index for 20/80 oil-in-water Pickering emulsions and for different particles concentrations. The less concentrated emulsion with just 0.1% (w/w) OS1 particles destabilized quickly with the phase separation reaching soon 80%. This means that the oil completely separated from the water which implies that particles around oil droplets offered limited protection against coalescence. As particles concentration increased, destabilization rate decreased and, in addition, the emulsion experienced lower degree of separation between the two phases. The much smaller than 80% final water fraction (at the time scale of observation) implies stabilization of the emulsion against coalescence leading to flocculation and creaming (see Section 5). Of course, coalescence may still occur but in a larger time scale.

When trying to compare volumetric with electrical measurements an important observation must be taken into account. For the 20/80 (v/v)/oil-in-water emulsion with 2.5% (w/w) particles the phase separation interface was below the two electrodes during all the measuring period. In other words, the electrodes were always submerged inside the cream (flocculated region). This was not so for the other emulsion compositions where the phase separation interface soon goes above the electrodes.

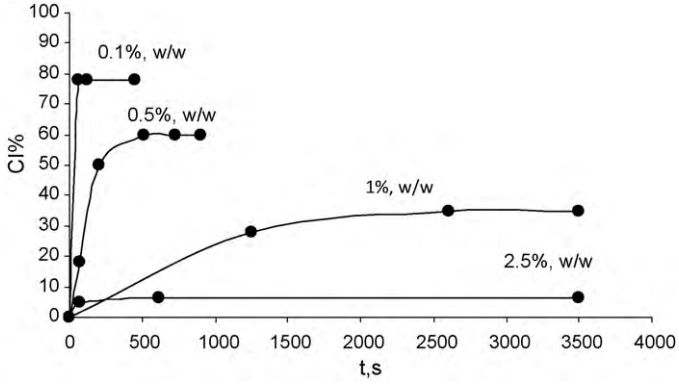


**Fig. 7.** Creaming index versus time for 20/80 oil-in-water Pickering emulsions.

### 3.3. Droplets size

Results obtained from the analysis of the microscope photographs are presented in Fig. 8. The Sauter mean diameter $d_{opt}$ of the emulsion from samples taken from the region of the electrical probe is shown against the solids concentration for the two emulsion compositions. In accordance with stability results from electrical and volumetric measurements, droplet size decreases as particle concentration increases. One would expect that droplet sizes would be smaller for the 40/60 than the 20/80 (v/v) oil-in-water emulsions. This is the case for 1% (w/w) particle concentration. For 0.5% (w/w), data points for the two emulsion compositions are close enough and can be considered comparable given the statistical lack of confidence (at a 95% level). For 0.1% and 2.5% (w/w) particles concentrations, the determination was statistically significant for a different composition each time so results for the other composition are not included in the plot.

## 4. Analysis of electrical conductance data

A detailed and realistic model of the destabilization procedure is very complex. Buoyancy velocity of each droplet is influenced from its neighbouring droplets. In addition to this motion, diffusion occurs (especially for small bubbles) simultaneously with coalescence due to gravitational and Brownian motion. The theoretical description of each from the above phenomena involves several parameters leaving many open issues to be resolved from experimental evidence. Even so, the computational cost for extensive parameter identification by fitting the model to experimental data is high. An example of such a model was formulated in [32] where several empirical parameters were employed in order to match the model with the experimental droplet size distributions. Due to the high computational cost the unknown parameter was found by inspection and not through a deviation minimization technique. The development of pressure build-up in a suspension of dense non-coalescing particles makes the modelling procedure even more complicated.

An alternative direct approach to extract problem parameters (droplet sizes and relative volume fractions) from electrical conductance data of the evolution of water volume fraction is developed here. In the following analysis, only the two main slopes in the water fraction evolution curves are considered as it is unknown at present what is the proper way to cope with other less pronounced slopes. Another issue of concern is the effect of coalescence between droplets during emulsion destabilization. If coalescence is dominant then the observed slopes represent integral information rather than specific droplet sizes. Our creaming index results show clearly that only for the case of 0.1% solids con-

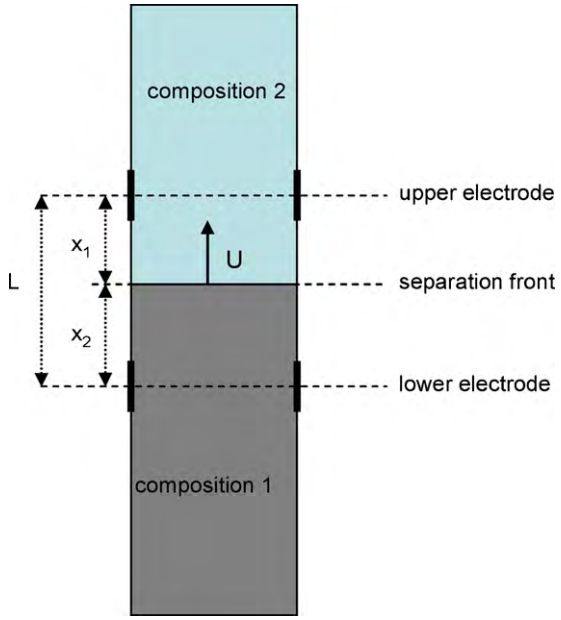


**Fig. 9.** Schematic and notation for the motion analysis of the phase separation front.

centration, particles are not enough to prevent droplets coalescence since the observed phase separation interface attains rapidly a position corresponding to total separation between oil and water. But even in this case it is reasonable to consider that only a very small degree of coalescence occurs up to the low height position of the electrodes pair in the vessel and coalescence is restricted to upper parts of the vessel where the oil phase accumulates. So, coalescence during emulsion destabilization is ignored in the analysis even for the lower solids concentration.

In order to develop a simple technique for the estimation of droplet sizes from the corresponding volume fraction evolution curve, the simple case of a moving front separating two phases with oil contents $\varphi_1$ and $\varphi_2$ is considered first. Let us assume that the "observation" volume is contained between the centres of the two electrodes. The distance between the centres of the two electrodes is denoted $L$ (Fig. 9). The motion of the front is upwards which implies that $\varphi_2 > \varphi_1$. The instantaneous distance between the front and the centre of the lower/upper electrode is $x_1/x_2$, respectively, such as $x_1 + x_2 = L$ (Fig. 9). Instead of solving the complete electrostatic problem, it is assumed that two resistances in series with conductivities given by the Bruggeman's law as $k_1 = k_w(1-\varphi_1)^{3/2}$ and $k_2 = k_w(1-\varphi_2)^{3/2}$ are contained between the electrodes. The average conductivity $k$ of the medium contained in the observation volume will be given according to the resistances in series model as:

$$k = \left(\frac{x_1}{k_1 L} + \frac{x_2}{k_2 L}\right)^{-1} \tag{4}$$

Inverting the procedure followed to create the experimental $\varphi$ versus $t$ curves based on the Bruggeman's equation leads to the following relation for $\varphi$, the oil volume fraction:

$$\varphi = 1 - \left(\frac{x_1}{(1-\varphi_1)^{3/2}L} + \frac{L-x_1}{(1-\varphi_2)^{3/2}L}\right)^{-2/3} \tag{5}$$

Assuming a constant velocity $U$ of the front motion and an initial condition $x = 0$ at an arbitrary time value $t_o$, the evolution equation for $\varphi$ takes the form ($t_o$ does not influence the analysis):

$$\varphi = 1 - \left(\frac{1}{(1-\varphi_2)^{3/2}} + \frac{U(t-t_o)}{L}\left(\frac{1}{(1-\varphi_1)^{3/2}} - \frac{1}{(1-\varphi_2)^{3/2}}\right)\right)^{-2/3} \tag{6}$$

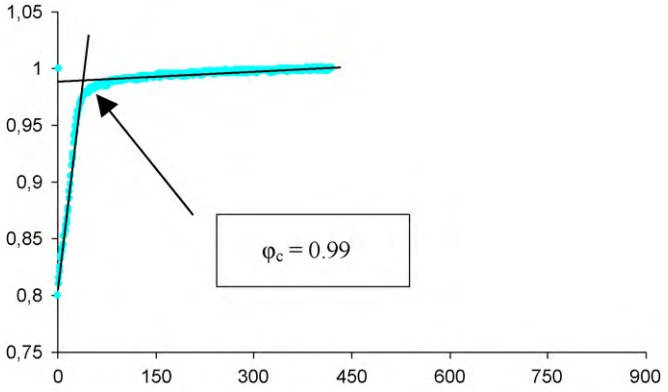


**Fig. 10.** Approximating the water fraction evolution curve by two straight lines.

The second term in the parentheses is in general smaller than the first term so expanding the power term in Taylor series and keeping only the first term leads to:

$$\varphi = \varphi_2 - (1-\varphi_2)\frac{2Ut}{3L}\left(1 - \left(\frac{1-\varphi_2}{1-\varphi_1}\right)\right)^{3/2} \tag{7}$$

Differentiating the above equation with respect to time and solving for the front velocity $U$ the following expression is derived relating the front velocity with the $\varphi(t)$ curve and with the characteristics of the phases separated by the front:

$$U = -\frac{d\varphi}{dt}\frac{3L}{2(1-\varphi_2)}\left(1 - \left(\frac{1-\varphi_2}{1-\varphi_1}\right)^{3/2}\right) \tag{8}$$

Assuming next a bidisperse distribution with small droplets having diameter $d_s$ and volume fraction $\varphi_s$ and large droplets having diameter $d_L$ and volume fraction $\varphi_L$ one can estimate the velocity $U_1$ of the front separating the initial dispersion from a dispersion containing only small droplets and the velocity $U_2$ of the front separating a dispersion containing small droplets from the continuous water phase as:

$$U_1 = \left(\frac{df_w}{dt}\right)_1 \frac{3L}{2(1-\varphi_s-\varphi_L)}\left(1 - \left(\frac{1-\varphi_s-\varphi_L}{1-\varphi_s}\right)^{3/2}\right) \tag{9}$$

$$U_2 = \left(\frac{df_w}{dt}\right)_2 \frac{3L}{2(1-\varphi_s)}(1-(1-\varphi_s)^{3/2}) \tag{10}$$

Subscripts 1 and 2 at the derivatives indicate the slope of the first and the second linear part of the experimental $f_w(t)$ curves. In practice there is no slope discontinuity at the intersection of the linear parts of the curves as the above theory predicts but instead a smooth transition from one part to the other. This is mainly due to the (ignored by the simplified model) sensitivity of the measured conductance to the front position when it is not between the electrodes. The nominal (based on the emulsion generation) volume fraction of oil is denoted as $\Phi = 1 - f_w(0)$. The procedure to determine the velocities $U_1$, $U_2$ and the oil volume fractions $\varphi_L$, $\varphi_s$ from the experimental curves is the following: First, the tangential lines at the two "linear" parts of the curve are drawn and their intersection point corresponding to a water content $\varphi_c$ is found (see Fig. 10 as an example). Then the volume fractions of the two oil components are computed as $\varphi_s = 1 - \varphi_c$ and $\varphi_L = \Phi - \varphi_s$, respectively. Finally, the corresponding velocities $U_1$ and $U_2$ are computed from the relations (9) and (10) using the slopes of the two tangential lines.

The next step is to relate the front velocities $U_1$ and $U_2$ to the corresponding droplet sizes $d_L$ and $d_s$. This is a problem in the core of the sedimentation theory. According to the general theories of polydisperse sedimentation [33] the velocity of each species (droplet

size) depends on the velocity of the other species. This interdependence of the two droplet sizes velocities can be ignored here since (i) regarding the first front, the small droplet velocity and volume fraction are too low to influence the velocity of large droplets and (ii) the second front occurs in the absence of large droplets. So the oil volume fraction for the first front is considered to be $\Phi$ and for the second front to be $\varphi_s$. What remains is to find a relation for the buoyancy velocity of a droplet at a specified dispersed phase volume fraction. The Stokes law for the buoyant velocity of droplets with immobile (due to the presence of solid particles) surface is taken as the starting point.

Regarding the influence of the volume fraction of the dispersed phase $\varphi$ on the buoyant velocity of droplets, the empirical relation of Richardson and Zaki was found as the most successful in correlating experimental data. It is just a correction of the form $(1-\varphi)^n$ to the drag force relation where n is the so-called Richardson–Zaki exponent. In many situations this empirical correlation was found compatible to theoretical expressions (for example $n = 6.5$ according to low $\varphi$ theory in [34]) but the value of n differs from experiment to experiment. It is a function of a single droplet's Reynolds number (based not on the real velocity but on that of an isolated droplet) and a correlation for this dependence is $n = (1.791 + 0.133\mathrm{Re}^{0.456})/(0.359 + 0.093\mathrm{Re}^{0.456})$ [35]. Of course this approach can be used only for approximate computations as it is the case here since the correlation for the exponent is not the only one and also there is a large scatter in the exponent values found by fitting experimental data. The Re number was taken into account for the dispersed phase concentration correction but not for the basic velocity computation. Fortunately, in the present experiments the single droplet Re number is always smaller than 1 so the Oseen correction to the Stokes drag law can be applied. Employing the Richardson–Zaki approach to the hindering effect of the oil volume fraction and the Oseen correction to the Stokes law yields the following relation for the buoyancy velocity ($u$ is the single droplet velocity and it is used in computation of Re):

$$u = \frac{(\rho_w - \rho_{oil})gd^2}{18\mu} \tag{11}$$

$$U = u(1 + 3Re/16)(1-\varphi)^{(1.791+0.133Re^{0.456})/(0.359+0.093Re^{0.456})} \tag{12}$$

Replacing the velocity values from the experimental results and the corresponding oil fractions for each velocity, the large and small droplet diameters $d_L$ and $d_s$ can be estimated.

## 5. Discussion

The droplet size distribution resulting from the emulsification procedure is the outcome of the simultaneous processes of coalescence between droplets and droplet breakage. The addition of particles reduces the coalescence process (stabilizing the water film between colliding droplets) and enhances the breakage process due to the reduction of the effective surface tension of the droplet in the presence of particles [36,37]. The combination of these effects results in the production of smaller droplets as particle concentration increases. Apart from controlling the droplet size during the emulsification stage, particles packed at the droplets interface can also affect the destabilization procedure. This can be done by increasing the apparent density of droplets and by making the interface immobile and rough. All these features retard the buoyant motion of droplets. However, in many cases the role of droplet size may be dominant over the other features. Finally, the oil fraction has a small effect on the emulsification process but it is important during the destabilization process, hindering the motion of oil droplets.

The volume fraction of small and large droplets ($\varphi_L$, $\varphi_s$), their diameters ($d_L$, $d_s$) as computed from electrical conductance measurements and the Sauter mean diameter of the droplet size distribution $d_{opt}$ as computed by microscopy observation are shown in Table 2. In general, $d_{opt}$ exhibits the same trends and appears to attain similar values (taking into account the completely different principles of the two techniques) with the large droplets of the bidisperse distribution estimated electrically. The two cases of low particle concentration 0.1% (for which the creaming index experiments revealed that coalescence occurs) exhibit a negligible to zero degree of bimodality whereas in the other cases (in which particles prevent coalescence) the degree of bimodality appears to be high. This behaviour is compatible with the well-known arguments that simultaneous coalescence and breakage leads to unimodal droplet size distributions [38] whereas breakage alone leads to bimodal (fragments-parent droplets) droplet size distributions [39]. Only the results for the case of 40/60 emulsion with 2.5% particles are incompatible to the whole picture. A unimodal distribution (instead of the expected bimodal one) with particles much smaller than $d_{32}$ is predicted by electrical measurements. The most pertinent explanation for this discrepancy is that in this particular case the electrodes were submerged all the time inside the flocculated region (cream) of the emulsion and under these conditions the destabilization kinetic can be much more complex from what has been considered in the present analysis of electrical signals.

It is noted that there is a threshold for particles concentration above which the water-oil interface becomes saturated with particles whereas the remaining particles stay dispersed in the continuous phase increasing radically its apparent viscosity by creating three-dimensional networks. This has a direct effect on the estimation of droplet size by the electrical technique which is based on droplets velocity. In general, ignoring an increased viscosity of the continuous phase would make the conductance technique estimate a smaller droplet size than the actual one. Based on the above, for concentrations lower than the threshold value particles stabilize the emulsion by controlling the droplet sizes created during emulsification. For larger than the threshold concentrations, an additional stabilization mechanism emerges: reduction of droplet mobility due to increase of the continuous phase viscosity. In the latter case, the analysis of electrical signals should incorporate the new viscosity in the data reduction procedure.

We have estimated the droplets coverage by individual particles from simple geometrical considerations based on the average droplet and particle sizes. It was found that particles were in excess for all examined particle concentrations i.e., from ~4 to ~40 times above the number required to saturate the droplets surface. Appar-

**Table 2**
Determination of droplet sizes and volume fractions via electrical curves and microscopy observations.

| Concentration of particles (OS1) (w/w) | Miglyol (%, v/v) | $\varphi_L$ | $d_L$ (μm) | $\Phi_s$ | $d_s$ (μm) | $d_{opt}$ (μm) |
|---|---|---|---|---|---|---|
| 0.1% | 20 | 0.19 | 113 | 0.01 | 26.4 | – |
| 0.5% | 20 | 0.18 | 73.4 | 0.02 | 23.9 | 78 |
| 1% | 20 | 0.12 | 61.5 | 0.08 | 13.28 | 68 |
| 2.5% | 20 | 0.2 | 16.4 | – | – | 50 |
| 0.1% | 40 | 0.4 | 112 | – | – | 100 |
| 0.5% | 40 | 0.36 | 54.3 | 0.04 | 15.22 | 82 |
| 1% | 40 | 0.35 | 43.3 | 0.05 | 7.56 | 60 |

ently, the highest excess was for the 2.5% particles concentration. However, for nano-sized particles usually a multilayer rather than individual particles covers droplets. If this is the case then it is perhaps not so strange that only for the 2.5% concentration there is a clear effect with the formation of 3D structures in the continuous phase capable of delaying droplets mobility.

All in all, electrical conductance measurements open new perspectives regarding the non-intrusive on-line (continuous) monitoring of emulsion destabilization. Electrical signals are representative of phenomena occurring across the entire cross-section of a vessel and not just the spot of immersing a sampling probe or the region of the walls. This is particularly useful when dealing with opaque emulsions and large diameter vessels (e.g. of industrial scale) where local information can be different from information averaged over the cross-section. In addition, combination of several electrodes along the height of a vessel allows tomographic type of measurements for the determination of the temporal and spatial evolution of phases distribution inside the vessel.

## 6. Conclusions

In the present work, three experimental techniques were used for the assessment of the stability of oil-in-water Pickering emulsions produced with different oil/water compositions and particles concentrations. Results from two classical techniques (the well-known volumetric measurement of phase separation and the optical measurement of droplet diameters from withdrawn samples) and a new technique (a non-intrusive on-line electrical conductance measurement of the local water fraction) were examined and compared to each other. The electrical technique, in addition to the direct assessment of the emulsion stability by monitoring the evolution of water fraction, can also be used for the estimation of droplet sizes assuming a bidisperse droplet size distribution and a negligible increase of the apparent viscosity of the continuous phase by the presence of particles. The droplet sizes estimated by analyzing conductance data were found to be comparable with those resulting from optical observations of the droplets. It is shown that the new electrical technique is advantageous over the volumetric and optical technique since it can offer information on fast local dynamic phenomena. The results and their discussion in this work reveal that the new technique is a tempting choice for studying emulsion destabilization where fast, non-intrusive, on-line measurements are required from the entire cross-section of a vessel and not just from a specific internal spot or the region of the walls.

## Acknowledgments

Financial support by the European Space Agency through the project FASES (Fundamental and Applied Studies of Emulsion Stability) (ESA-AO-2004-PCP-109/ELIPS-2) is gratefully acknowledged. This work was conducted under the umbrella of the COST P21 action: Physics of Droplets.

## References

[1] B.P. Binks, Modern Aspects of Emulsion Science, The Royal Society of Chemistry, Cambridge, 1998.
[2] H. Schubert, H. Armbruster, Int. Chem. Eng. 32 (1992) 14.
[3] M.J. Rosen, Surfactants and Interfacial Phenomena, John Wiley & Sons, New York, 1978.
[4] S. Friberg, K. Larsson, J. Sjoblom, Food Emulsions, Marcel Dekker, New York, 2004.
[5] W. Ramsden, Proc. R. Soc. 72 (1903) 156–164.
[6] S.U. Pickering, J. Chem. Soc. 91 (1907) 2001–2021.
[7] B.P. Binks, Curr. Opin. Colloid Interface Sci. 7 (2003) 21–41.
[8] T.N. Hunter, R.J. Pugh, G.V. Franks, G.J. Jameson, Adv. Colloid Interface Sci. 137 (2008) 57–81.
[9] A. Drelich, F. Gomez, D. Clausse, I. Pezron, Stability of water-in-oil emulsions prepared with solid particles. Influence of added emulsifier, in: 4th International Workshop "Bubble and Drop Interfaces", September 23rd–25th, Thessaloniki, Greece, 2009.
[10] C.P. Whitby, D. Fornasiero, J. Ralston, J. Colloid Interface Sci. 329 (1) (2009) 173–181.
[11] M.C. Sanchez, M. Berjano, A. Guerrero, C. Gallegos, Langmuir 17 (18) (2001) 5410–5416.
[12] T. Goloub, R.J. Pugh, J. Colloid Interface Sci. 257 (2003) 337–343.
[13] C. Desnoyer, O. Masbernat, C. Gourdon, Chem. Eng. Sci. 58 (7) (2003) 1353–1363.
[14] M.M.M. Ribeiro, M.M.L. Guimaraes, C.M.N. Madureira, J.J.C. Cruz Pinto, Chem. Eng. J. 97 (2) (2004) 173–182.
[15] S. Sajjadi, Langmuir 22 (13) (2006) 5597–5603.
[16] L. Pakzad, F. Ein-Mozzafari, P. Chan, Chem. Eng. Sci. 63 (9) (2008) 2508–2522.
[17] E. Fransolet, M. Crine, P. Marchot, D. Toye, Chem. Eng. Sci. 60 (22) (2005) 6118–6123.
[18] G.P. Lucas, J. Cory, R.C. Waterfall, W.W. Loh, F.J. Dickin, Flow Meas. Instrum. 10 (1999) 249–258.
[19] F. Ricard, C. Brechtelsbauer, X.Y. Xu, C.J. Lawrence, Chem. Eng. Res. Des. 83 (7) (2005) 794–805.
[20] D. Vlaev, M. Wang, T. Dyakowski, R. Mann, B.D. Grieve, Chem. Eng. J. 77 (1–2) (2000) 87–91.
[21] M. Kaminoyama, S. Taguchi, R. Misumi, K. Nishi, Chem. Eng. Sci. 60 (20) (2005) 5513–5518.
[22] N.A. Tsochatzidis, T.D. Karapantsios, M.V. Kostoglou, A.J. Karabelas, Int. J. Multiphase Flow 18 (1992) 653–667.
[23] T.D. Karapantsios, N.A. Tsochatzidis, A.J. Karabelas, Chem. Eng. Sci. 48 (8) (1993) 1427–1436.
[24] T.D. Karapantsios, E.P. Sakonidou, S.N. Raphaelides, Carbohydr. Polym. 49 (4) (2002) 479–490.
[25] T.D. Karapantsios, M. Papara, Colloids Surf. A: Physicochem. Eng. Aspects 323 (1–3) (2008) 139–148.
[26] M. Papara, X. Zabulis, T.D. Karapantsios, Chem. Eng. Sci. 64 (2009) 1404–1415.
[27] A. Bumajdad, J. Eastoe, J. Colloid Interface Sci. 274 (1) (2004) 268–276.
[28] J. Allouche, E. Tyrode, V. Sadtler, L. Choplin, J.-L. Salager, Langmuir 20 (6) (2004) 2134–2140.
[29] M. Rondón-González, L.F. Madariaga, V. Sadtler, L. Choplin, L. Márquez, J.-L. Salager, Ind. Eng. Chem. Res. 46 (2007) 3595–3601.
[30] E.P. Kalogianni, E.-M. Varka, T.D. Karapantsios, M. Kostoglou, E. Santini, L. Liggieri, F. Ravera, Colloids Surf. A: Physicochem. Eng. Aspects 354 (1–3) (2010) 353–363.
[31] X. Zabulis, M. Papara, A. Chatziargyriou, T.D. Karapantsios, Colloids Surf. A: Physicochem. Eng. Aspects 309 (2007) 96–106.
[32] R. Cunha, M. Fortuny, C. Dariva, A.F. Santos, Ind. Eng. Chem. Res. 47 (2008) 7094–7103.
[33] S. Berres, R. Burger, E.M. Torry, Chem. Eng. J. 111 (2005) 105–117.
[34] G.K. Batchelor, J. Fluid Mech. 52 (1972) 245–268.
[35] A.V. Nguyen, H.J. Schulze, Colloidal Science of Flotation, Marcel Dekker, New York, 2004.
[36] P.S. Clegg, E.M. Herzig, A.B. Schofield, T.S. Horozov, B.P. Binks, M.E. Cates, W.C.K. Poon, J. Phys.: Condens. Matter 17 (2005) 3433–3438.
[37] B.P. Binks, Curr. Opin. Colloid Interface Sci. 7 (2002) 21–41.
[38] M. Kostoglou, A.J. Karabelas, J. Aerosol Sci. 30 (1999) 157–162.
[39] M. Kostoglou, A.J. Karabelas, Chem. Eng. Sci. 60 (2005) 6584–6595.